Dual Structural Requirements for Multilineage Hematopoietic-Suppressive Activity of Chemokine-Derived Peptides[†]

L. Lecomte-Raclet,[‡,#] M. Rholam,[§,#] M. Alemany,[‡] N. Lazar,[§] C. Simenel,[‖] M. Delepierre,[‖] Z. C. Han,[⊥] P. Cohen,[§] and J. P. Caen*,[‡]

Hôpital Lariboisière, Institut des Vaisseaux et du Sang, 8 rue Guy Patin, 75475 Paris, France, Unité Mixte de Recherche 7631 CNRS, Université Pierre et Marie Curie, 96 bd Raspail, 75006 Paris, France, CNRS−URA 2185, Biologie structurale et agents infectieux, Institut Pasteur, 28 rue du Dr Roux, 75724 Paris, France, and Key Laboratory of Hematology, Institute of Hematology, Tianjin, China

ABSTRACT: Many chemokines have direct suppressive activity in vitro and in vivo on primitive hematopoietic cells. However, few chemokine-derived peptides have shown a significant activity in inhibiting hematopoiesis. Interestingly, a peptide derived from the 34−58 sequence of the CXC chemokine platelet factor 4 (PF4) produced a 30−40% inhibition of proliferation of murine hematopoietic progenitors (CFU-MK, CFU-GM, and BFU-E) in vitro, at concentrations of 30−60-fold lower than PF4. The aim of the present work was to define the structural parameters and motifs involved in conferring biological activity to the peptide PF4(34−58). Both structural predictions and determinations revealed a new helical motif that was further localized between residues 38 and 46. This helix was necessary for binding of the peptide and for permitting the functional DLQ motif at position 54−56 to activate the putative receptor site. Peptides lacking either the helical or the DLQ motif were devoid of inhibitory activity on the hematopoietic progenitors in vitro. However, among inactive peptides, only those having the helical motif counteracted the inhibition induced by the active peptide PF4(34−58). This suggested that the helix might be required for peptide interactions with a putative receptor site, whereas the DLQ motif would be implicated in the activation of this receptor. These results identify for the first time the dual requirements for the design of chemokine-derived peptides with high suppressive activity on hematopoiesis, as well as for the design of molecules with antagonistic action.

Chemokines are 70−80-residue proteins containing 4 conserved cysteines. On the basis of the relative position of the two first cysteines (*1*), these molecules were subdivided into four families, designated CXXXC, CXC, CC, and C. They have been implicated in different activities, including modulation of inflammation, hemostasis, angiogenesis, and cell proliferation. In addition, some chemokines possess an inhibitory activity toward the proliferation of immature hematopoietic stem and progenitor cells in vitro and in vivo (*2*−*5*). This hematopoietic-suppressive activity has been demonstrated for some CXC chemokines, such as platelet factor 4 (PF4),[1] interleukin-8 (IL8), macrophage inflamma-

tory protein-2α (MIP-2α), and γ-interferon-inducible protein (IP10), as well as for the CC chemokine MIP-1α. The molecular mechanisms underlying the growth-inhibitory effects of these chemokines are not yet well-understood. Therefore, structure(s)−function(s) studies of these cytokines will be helpful in determining the mechanism(s) by which these chemokines act on hematopoiesis.

CXC chemokines exhibit high homology in amino acid sequences (20−45%), especially in the carboxy-terminal region which confers basic heparin-binding activities to these proteins. Three-dimensional conformations of PF4 and many other CXC chemokines have been solved and show general structural identity (*6*, *7*). Each monomer has a flexible N-terminal region followed by three antiparallel β-strands and a carboxy-terminal α-helix. The ELR motif of the IL8 ligand has been shown to be required for specific interaction with either of the two IL8 receptor proteins on the surface of neutrophils (*8*−*10*). The ELR motif is conserved in all IL8-related chemokines with neutrophil activating properties, but not in PF4, IP10, or CC chemokines. Instead, PF4 contains the DLQ motif, which has been shown to be required for the activity of this chemokine. Two copies of this DLQ motif are located at positions 7−9 and 54−56 of the PF4 sequence. Receptors for almost all chemokines have been identified and shown to be classical seven-transmembrane-domain receptors coupled to G protein (*11*). In contrast,

---

* To whom correspondence should be addressed. Tel: +33 1 45 26 21 98. Fax: +33 1 42 82 94 73. E-mail: jcaenivs@club-internet.fr.
‡ Institut des Vaisseaux et du Sang.
§ Université Pierre et Marie Curie.
‖ Institut Pasteur.
⊥ Institute of Hematology.
# These authors contributed equally to this work.

[1] Abbreviations: AAS, aplasic anemia serum; BSA, bovine serum albumin; CD, circular dichroism; CSI, chemical shift index; IL8, interleukin-8; IP10, γ-interferon-inducible protein 10; MIP, macrophage inflammatory protein; PF4, platelet factor 4; rmGM-CSF, recombinant murine granulocyte-macrophage colony stimulating factor; rmIL-3, recombinant murine interleukin-3; rmSCF, recombinant murine stem cell factor; TFA, trifluoroacetate; TFE, trifluoroethanol.

Table 1: Amino Acid Sequences of PF4(34−58)-Related Peptide Substrates[a]

peptides		sequence
reference	PF4(34−58)	PHSPTAQLIATLKNGRKISLDLQAP
A	PF4(37−58)	PTAQLIATLKNGRKISLDLQAP
	[Ala37,Pro39](34−58)	PHSATPQLIATLKNGRKISLDLQAP
	[Ala37](34−58)	PHSATAQLIATLKNGRKISLDLQAP
	[Ala34,Ala37](34−58)	AHSATAQLIATLKNGRKISLDLQAP
B	PF4(34−56)	PHSPTAQLIATLKNGRKISLDLQ
	PF4(34−53)	PHSPTAQLIATLKNGRKISL
	PF4(34−58)DLE	PHSPTAQLIATLKNGRKISLDLEAP
	PF4(34−58)DLN	PHSPTAQLIATLKNGRKISLDLNAP

[a] Modifications in the N-terminal (A) and in the C-terminal (B) regions are underlined.

PF4 has not been shown yet to bind to any characterized chemokine receptor, with the possible exception of the Duffy antigen (*12*).

In the last few years, several efforts have been made in the study of active chemokine-derived peptides, as well as of antagonistic molecules in the nanomolar range. For instance, several linear and cyclic peptides corresponding to the N-terminal sequence of IL8, NAP2, or PF4 have been tested, but none had functional activity at concentrations under the millimolar range (*13*); neither were they active in a receptor-binding assay (*8, 13*). Significant inhibition of hematopoiesis was observed with peptides derived from the C-terminal region of PF4, but only when used at high concentrations, and the effect was reversed in the presence of heparin.

The ability of the derived peptides to retain the full activity of the whole molecule is usually limited by the loss of the native functional structure. In a recent study it was shown that a peptide corresponding to the 34−58 sequence of PF4 inhibited myeloid colony formation at concentrations as low as 22 nM; that is, 30 times lower for CFU-MK and 60 times lower for CFU-GM and BFU-E than those required for the intact PF4 molecule (*14*). We report here on the structural characterization and activity of several modified PF4(34− 58) peptides which were designed to identify the sequences and structural motifs implicated in the hemosuppressive activity of the peptide. Moreover, some of the described peptides may have interesting applications as agonists or antagonists of chemokine activities.

EXPERIMENTAL PROCEDURES

Reagents and Growth Factors. Recombinant murine granulocyte-macrophage colony stimulating factor (rmGM-CSF) was provided by Beite Kaito (Paris, France), and recombinant murine stem cell factor (rmSCF) and recombinant interleukin-3 (rmIL-3) were provided by R & D (Oxford, United Kingdom). Both growth factors were diluted in PBS + 0.01% bovine serum albumin (BSA) and stored at −20 °C. 2,2,2-Trifluoroethyl alcohol-d_2,OH (99 atom %D) and deuterium oxide (99.97 atom %D) were purchased from Euriso-top (CEA, France).

Peptide Synthesis. Peptides were synthesized using Merrifield solid-phase methodology (*15*) and purified by HPLC using a C_{18} column and a 0−80% linear acetonitrile gradient in 0.1% trifluoroacetic acid (TFA). Amino acid sequences of the peptides are shown in Table 1. The concentration of

PF4(34−58) peptides was determined through mass estimation and amino acid analysis.

Colony Assays of Hematopoietic Progenitors

Cell Preparation. Total bone marrow cells obtained from Balb/c mice were used in the present study. The mice, 6−8-week-old males, were purchased from IFFA CREDO Laboratories (L'Arbresle, France) and maintained under standard housing conditions with water and commercial rodent chow. After the mice were killed by cervical dislocation, the femurs were removed and the total bone marrow was expelled with 5 mL α-medium (Eurobio, Paris, France).

CFU-MK Assay. Megakaryocytes and their progenitor cells were studied using a plasma clot system (*14*). Briefly, 2×10^5 nucleated marrow cells were cultured in triplicate in Petri dishes (35 mm) in a total volume of 1 mL containing 1% BSA (Sigma, St. Quentin Fallavier, France), 10% bovine citrated plasma (GibCo, Cergy-Pontoise, France), 1×10^{-4} M 2-mercaptoethanol (Sigma), 0.34 mg $CaCl_2$ (Prolabo, Paris, France), 15 U penicillin plus 15 μg streptomycin, and 10% pig aplasic anemia serum (AAS). Synthetic peptides were incubated at 37 °C in a humidified atmosphere of 5% CO_2. After 7 days of incubation, the dishes were fixed, using 1% paraformaldehyde, and stained for acetylcholinesterase to determine the number of colonies derived from CFU-MK. Identification of colonies was performed as previously described (*14*). A CFU-MK-derived colony was defined as a group of three or more cells. Megakaryocytes and CFU-MK were counted using a computerized automatic image analysis (*16*). Briefly, the analysis system was based on acetylcholinesterase staining, specific stain for murine bone marrow megakaryocytes, and an image-capturing instrument equipped with a computer program.

BFU-E and CFU-GM Assays. BFU-E and CFU-GM were assayed using a methycellulose system as previously described (*14*). 1×10^5 nucleated marrow cells/mL were plated in a semisolid medium containing 0.8% methylcellulose, 10% AAS, 1×10^{-4} M 2-mercaptoethanol, 10 ng/mL rmSCF, 10 ng/mL rmGM-CSF, and 10 ng/mL rmIL-3 for BFU-E and CFU-GM assays. Quadruplicate cultures for each assay were incubated at 37 °C in a humidified atmosphere of 5% CO_2. BFU-E colonies (≥3 clusters of 20 cells each) and CFU-GM colonies (≥50 cells) were counted under an inverted microscope after 5 days of incubation.

Statistical Analysis. Results were expressed as the mean ±SEM for data from 3 or more separate experiments.

Secondary Structure Prediction. Predictions of the helical content of the PF4-derived peptides were performed using the AGADIR algorithm (*17*). This procedure allows calculation of the helicity per residue and the total helicity of the peptides, while considering short-range interactions in different conditions of solvent, temperature, and pH.

Circular Dichroism. Circular dichroic (CD) spectra were recorded on a Jobin-Yvon Mark IV which was linked to a PC microprocessor. Optical cells were placed in a thermostable cell holder. Measurements in the far-UV (190−250 nm) range were performed either in H_2O or in an H_2O/trifluorethanol (TFE) mixture. Spectra were the average of five consecutive scans recorded at a scan rate of 0.2 nm/s.

Measured spectra were corrected for the buffer baseline and were smoothed. Results are expressed as mean residue

ellipticity $[\theta]_R$ (deg·cm²·dmol⁻¹), which is related to the molar circular dichroism $\Delta\epsilon$ by the following relationship: $[\theta]_R = (3298 \times \Delta\epsilon)/N$, where N is the number of residues. Analysis for prediction of secondary structures from the CD recorded spectra was performed as described elsewhere (*18*).

Fourier Transform-Infrared Spectroscopy. Infrared spectra were recorded using a Bomem FTIR spectrometer (MB-series) which was linked to a PC microprocessor. The peptides were placed at 25 °C into an infrared cell with CaF₂ plates and a 50-μm path-length spacer. For each spectrum, 50 scans were collected at resolution of 4 cm⁻¹ and were added. During data acquisition, the spectrometer was continuously purged with dry N₂ to eliminate the spectral contribution of atmospheric water. Prior to sample preparation, the TFA counterions were discarded as described elsewhere (*19*) in order to eliminate their strong C=O stretching-absorption band near 1673 cm⁻¹. Measurements were performed in D₂O/TFE-d_2 mixtures (25 and 50%) for peptide concentrations of 10 mg/mL.

Prior to curve fitting, a straight baseline passing through the ordinates at 1750 and 1500 cm⁻¹ was subtracted. Second-derivative spectra, accompanied by 5-data-point Savitsky−Golay smoothing, were calculated in order to identify the positions of the component bands in the spectra (*20*). These wavenumbers were used as initial parameters for curve fitting with Gaussian component peaks. Position, bandwidth, and amplitude of the peaks were varied until (i) the resulting bands shifted by no more than 2 cm⁻¹ from the initial parameters, (ii) all of the peaks had reasonable half-widths (<20−25 cm⁻¹), and (iii) good agreement between the calculated sum of all components and the experimental spectra was achieved ($r^2 > 0.99$).

The obtained components (amide I band) were assigned to particular structures on the basis of several reports (*20−23*), and their relative contents were estimated by dividing the areas of individual peaks by the whole area of the resulting amide I band.

Proton NMR Experiments. The samples were solubilized in 10 mM aqueous buffer at pH 7. The measured pH values after the samples' dissolving varied between 5.1 and 6.1. TFE-d_2 was then added to obtain a 20% v/v TFE-d_2/H₂O solution. The final peptide concentrations varied from 2.2 to 3.5 mM.

All NMR measurements were obtained on a Varian Unity 500, later upgraded to INOVA, spectrometer operating at a proton frequency of 500 MHz and interfaced to a Sun Ultra station. The sweep width was 5000 Hz. Spectra in TFE /H₂O mixtures were recorded at 25 °C and referenced to the internal residual methylene resonance of TFE-d_2 at 3.95 ppm relative to external DSS at 0 ppm.

The OH-resonance of H₂O or of TFE-d_2 was suppressed by selective irradiation during the relaxation delay, and in the case of NOESY during the mixing time, as well, using the transmitter in the coherent mode (*24*). All 2D-data were collected in the phase-sensitive mode using the States−Haberkorn method (*25*). A total of 400−512 FIDS of 2K complex data points were collected in t_2 with 16−32 scans/increment, and zero-filling was applied in both dimensions prior to Fourier transformation to form a matrix of 4K × 2K. These data were then processed with shifted sine-bell window functions in both dimensions.
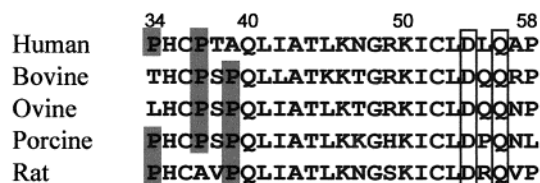

FIGURE 1: Alignment of the PF4 sequence 34−58 derived from different species. Prolines forming the motif Pro³⁴-(Xaa)$_n$-Pro³⁵⁺ⁿ are highlighted. Open boxes indicate the Asp⁵⁴-Xaa-Gln⁵⁶ motif for each species (*31−35*).

The phase-sensitive two-dimensional double-quantum-filtered correlated spectroscopy (DQF-COSY) (*26*) and total correlated spectroscopy (clean-TOCSY) (*27, 28*) were used for spin-systems assignment. The TOCSY experiment employed an MLEV-17 pulse sequence for the spin-lock and 80 ms mixing time with an effective radio-frequency field strength of 10 kHz. NOESY experiments (*29*) using a mixing time of 300 ms were recorded for sequential assignment and structure determination. ³$J_{NH-H\alpha}$ coupling constants were measured from DQF-COSY using a digital resolution of 1.25 Hz/pts.

Total helical content was obtained from conformational shifts calculated by adding all α-proton upfield shifts in helical segments, divided by the total number of peptide bonds and 0.38 ppm, which is the average value estimated for 100% helicity (*30*).

RESULTS

Analysis of the PF4(34−58) amino acid sequence among five different species (Figure 1) reveals the existence of a highly conserved 40−53 segment containing only three mutations at positions 45, 47, and 49 flanked on its N- and C-termini by two variable motifs: the Pro³⁴-(Xaa)$_n$-Pro³⁵⁺ⁿ pattern ($n \leq 4$) and the Asp⁵⁴-Xaa-Gln⁵⁶ tripeptide (DXQ motif), respectively. The DLQ motif was shown to be essential for the suppressive activity of the human PF4 molecule (*36*), whereas the Pro-(Xaa)$_n$-Pro patterns were observed in many biologically important peptide and protein sequences (*38−40*). Because it was observed that the PF4-(34−58) peptide inhibits the proliferation of progenitor cells at concentrations 30−60-fold lower than the PF4 molecule (*14*), we speculated that both the motifs and the central sequence might participate in the inhibitory effect of the PF4-(34−58) peptide.

Secondary Structure of the PF4(34−58) Peptide. In an attempt to characterize the structural parameters which might be involved in biological activity of the PF4(34−58) peptide, the AGADIR method (*17*) was used to predict the helical propensity of PF4(34−58)-derived peptides.

Noticeably, the 34−39 sequence contains two conserved proline residues separated by either one, two, or four different amino acids. Considering the peculiar properties of this amino acid residue in proteins (*38*), we have investigated the secondary structure of human PF4(34−58) peptides in which the motif Pro³⁴-(Xaa)$_n$-Pro³⁵⁺ⁿ was either deleted or its size (n) varied. Figure 2A indicates that when the number of amino acid residues separating the two prolines increases ($2 \leq n \leq 4$) or when the N-terminal sequence is deleted, the helicity values per residue of the resulting peptides decrease. However, it could be observed that the size of the Pro³⁴-(Xaa)$_n$-Pro³⁵⁺ⁿ motif produced the largest effect. In-
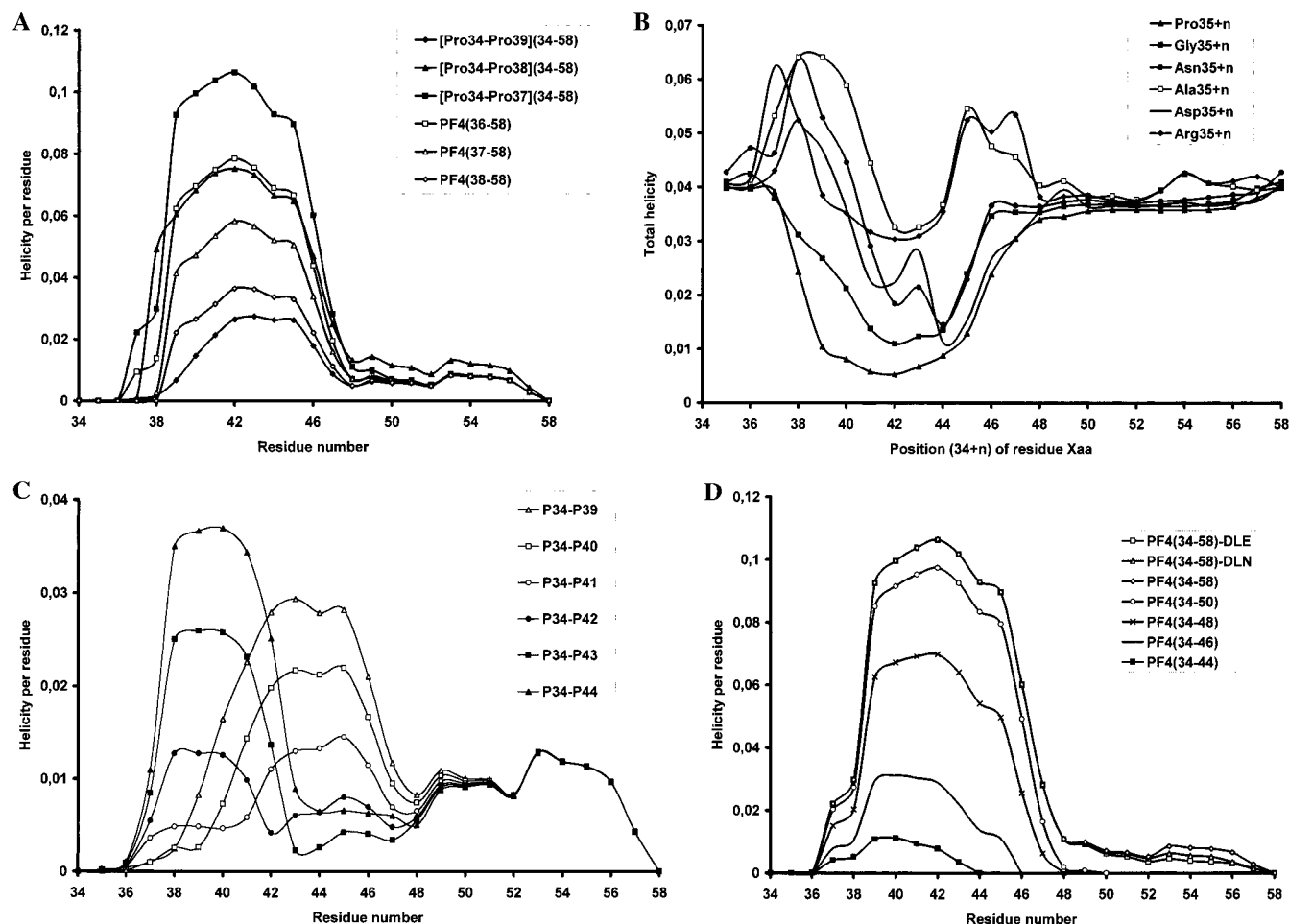
FIGURE 2: Secondary structure prediction of PF4(34−58) peptide. (A) Helicity per residue calculated for peptides with Pro^{34}-$(Xaa)_n$-Pro^{35+n} motifs ($4 \geq n \geq 2$) or truncated on the NH_2-terminal. (B) Variation of the total-helicity value of peptides with Pro^{34}-$(Xaa)_n$-Zaa^{35+n} motifs. (C) Helicity per residue calculated for motif peptides exhibiting lower total-helicity values. (D) Helicity per residue calculated for peptides in which the DLQ motif was either deleted or modified.

terestingly, lower values of the helicity per residue were obtained for both the porcine and rat PF4(34−58) peptides, which contain the Pro^{34}-$(Xaa)_4$-Pro^{39} pattern (Figure 1). These observations suggest that the Pro^{34}-$(Xaa)_2$-Pro^{37} motif plays a key role in the conformation adopted by the human PF4-(34−58) peptide, either by participating in the stability of its conformation or by favoring an adequate conformation involved in its biological activity.

As shown in Figure 2A, the peptide helicity of the PF4-(34−58) molecule was mainly due to the nature of the 38−48 segment. In an attempt to determine the role of this particular fragment, we investigated the secondary structure of PF4(34−58) peptides in which the residue Pro^{37} was shifted at different positions. Figure 2B indicates that when this residue shifts toward the C-terminal, the total helicity value of the resulting peptide decreases, reaches a minimum for proline at positions 41−42, and then increases to return to its original value. Moreover, the helicity value per residue, which followed the same variation as the total helicity, revealed that the constraints introduced by the proline residue vary, depending upon its position within the 38−48 sequence (Figure 2C). This conclusion was reinforced by the replacement of Pro^{35+n} by alanine (a strong α-helix promoter), which induced a marked effect on the calculated total peptide helicity of PF4(34−58) peptides with motifs Pro^{34}-$(Xaa)_n$-Ala^{35+n} (Figure 2B). Furthermore, comparison of the variation

of the total peptide helicity values for the peptides with motifs Pro^{34}-$(Xaa)_n$-Zaa^{35+n} (Zaa = Pro, Gly, Ala, Arg, or Asp, for example) revealed the following: (i) proline residue in position 35+n plays a key role in conformation of PF4-(34−58)-derived peptides, and (ii) the AGADIR method detects the existence of two helical segments in the PF4-(34−58) peptide which are located on both sides of the minimum (positions 41−42) observed for the total helicity of the Pro^{34}-$(Xaa)_n$-Ala^{35+n} motif (Figure 2B) or the helicity per residue of the Pro^{34}-$(Xaa)_n$-Pro^{35+n} motif (Figure 2C).

Because of the importance of the DLQ motif in the biological activity of both the human PF4 molecule (*36*) and the PF4(34−58) peptide (*14*), the secondary structure of PF4-(34−58) analogues in which this motif was either deleted or modified was also explored. Figure 2D indicates that deletion of the C-terminal Ile^{51}−Pro^{58} sequence (the sequence containing the DLQ motif) produced only small variations in the helicity values per residue of the PF4(34−50) peptide. Interestingly, the same effects were also observed for the PF4(34−58) peptides in which the DLQ motif was modified. Together, these results suggest that although the DLQ motif is involved in the biological activity of the PF4(34−58) peptide, the C-terminal Ile^{51}−Pro^{58} sequence probably does not participate in the secondary structure of this peptide. Alternatively, this sequence containing the DLQ motif might constitute an independent domain.
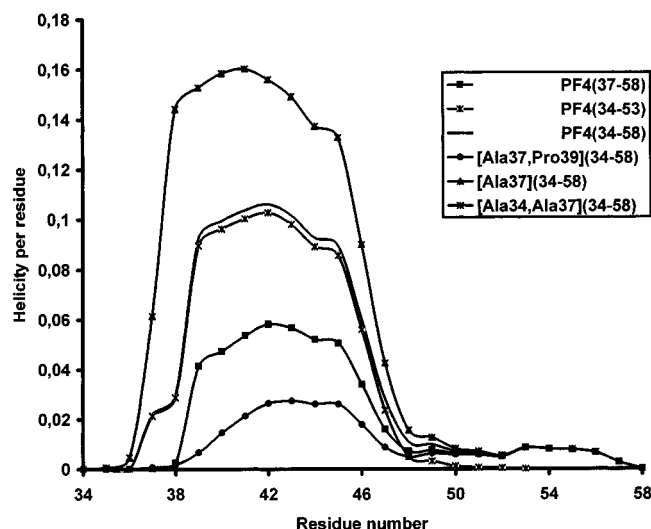
FIGURE 3: Secondary structure predictions of PF4(34−58) peptides tested in inhibition assays. The helicity per residue values calculated by the AGADIR method were plotted as a function of the residue number. The various peptides are described in Table 1.

On the basis of these considerations, different PF4(34−58)-derived peptides were designed and synthesized (Table 1). Both their biological activity and their secondary structure were measured and compared to those of the reference PF4-(34−58) peptide.

Biological Activity of PF4(34−58) Peptide Derivatives. The predicted secondary structure of synthetic peptides (Figure 3), using the Agadir method, clearly underlined large differences in their propensity to organize helical structure. Accordingly, the inhibitory activity of those peptides was examined in a proliferation assay for murine hematopoietic progenitors in order to test the hypothesis that this type of secondary structure and/or other parameters might participate in the biopotency of the corresponding molecules.

Importance of the N-Terminal Motif. Analysis of data in Figure 4A−C revealed large differences in the biopotency of peptides [Ala^{37},Pro^{39}](34−58), [Ala^{37}](34−58), [Ala^{34},Ala^{37}](34−58), and PF4(37−58). Whereas a 22 nM concentration of the PF4(34−58) peptide was required to exert a significant inhibitory effect on the number of CFU-GM, CFU-MK, and BFU-E cells, it was found that doses as high as 10-fold of that of peptide [Ala^{37},Pro^{39}](34−58) were needed to produce the same effect. Moreover, deletion of the N-terminal Pro^{34}−Ser^{36} tripeptide sequence decreased by a factor of 30 the inhibitory activity of the PF4(37−58) peptide in the same proliferation test. Together, these observations underlined the importance of the Pro^{34}-(Xaa)$_2$-Pro^{37} motif in favoring an optimal peptide conformation for a suppressive activity of the progenitor cells. When the peptides [Ala^{37}](34−58) and [Ala^{34},Ala^{37}](34−58) were tested, it was observed in contrast that 100-fold lower doses were sufficient to inhibit the proliferation of progenitor cells (Figure 4A−C). Because replacement of Pro^{39} by Ala^{39} in the peptide [Ala^{37},Pro^{39}](34−58) amplified considerably the biopotency of those resulting molecules, these data strongly suggest that the helical structure of the peptide segment comprised between residues 34 and 47 (Figure 2B) appeared to be essential for their activities. This conclusion is supported by the differences observed for the predicted secondary structures of those peptides (Figure 3).
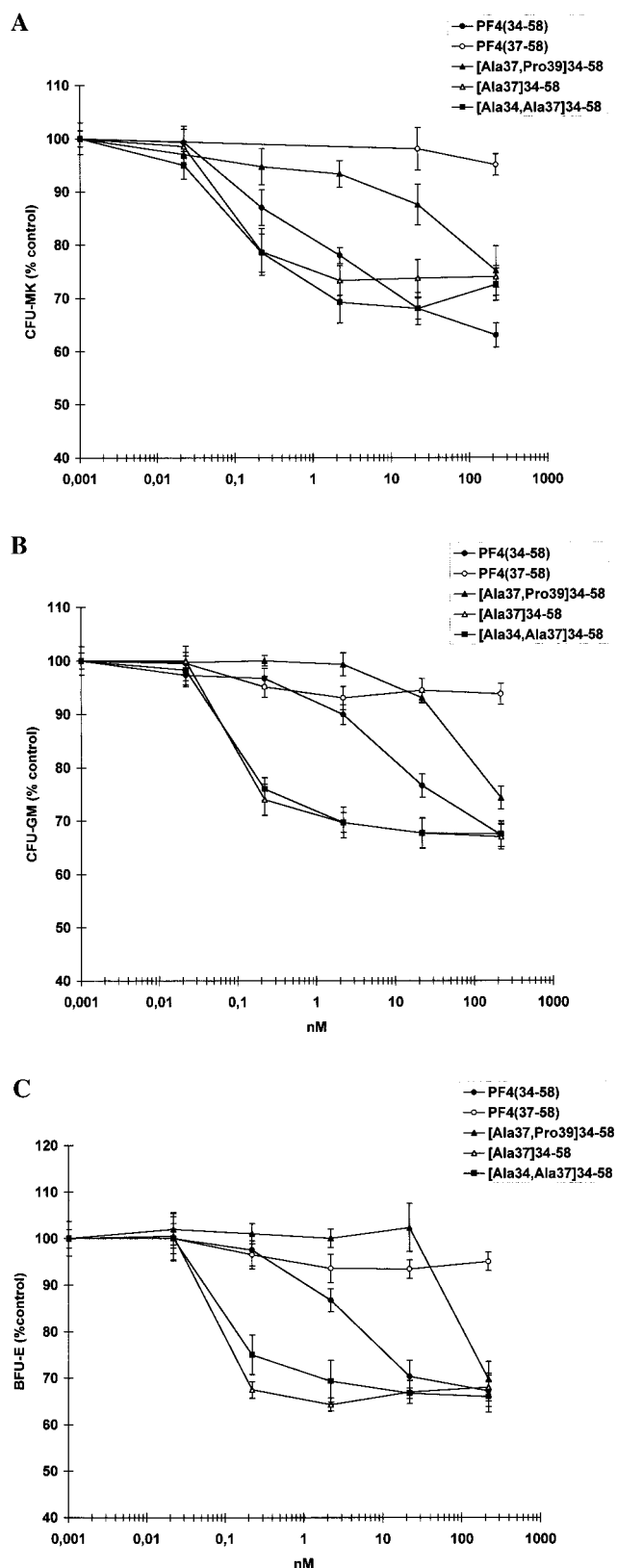

FIGURE 4: Structure−function relationship of the N-terminal α-helix of peptide PF4(34−58). Effect of a dose range of PF4(34−58) analogues on the proliferation of CFU-MK (A), CFU-GM (B), and BFU-E (C) colonies. Values are expressed as mean ± SEM of quadruplicate determinations obtained from three separate experiments. One hundred percent (100%) corresponds to the number of colonies derived from CFU-MK colonies (75 colonies/2 × 10^5 cells plated for culture), CFU-GM (84 colonies/1 × 10^5 cells plated for culture), and BFU-E (64 colonies/1 × 10^5 cells plated for culture) in nontreated control cultures.
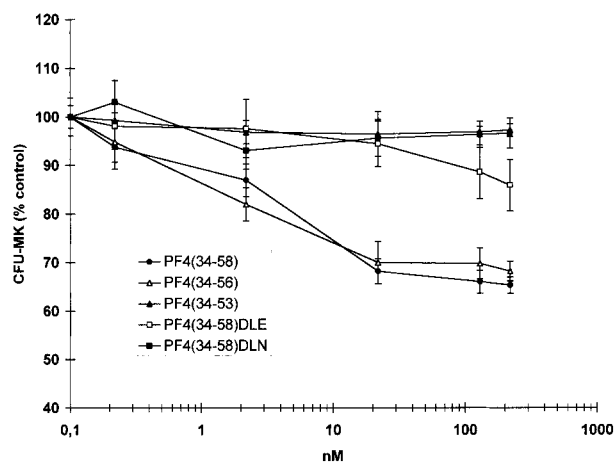
FIGURE 5: Structure−function relationship of the C-terminal DLQ motif of the peptide PF4(34−58). Effect of a dose range of peptides with C-terminal deletions or modified DLQ on the proliferation of CFU-MK colonies. Culture and determination of the number of CFU-MK colonies was performed as described under Figure 4. One hundred percent (100%) corresponds to the number of colonies derived from CFU-MK colonies (75 colonies/2 × 10^5 cells plated for culture) in nontreated control cultures. Similar inhibition profiles for each peptide were obtained for both CFU-GM and BFU-E.

FIGURE 6: Respective roles of the α-helix and the DLQ motif in the PF4(34−58) peptide. For the competition assay, cultures were grown in the presence of 22 nM of the active, reference peptide PF4(34−58), mixed with an excess of a modified inactive peptide (22 to 220 nM). Culture and determination of the number of CFU-MK colonies was performed as described under Figure 3. One hundred percent (100%) corresponds to the number of CFU-MK colonies (70 colonies/2 × 10^5 cells plated for culture) in nontreated control cultures. *$P < 0.01$ vs control cultures in the absence of any peptide.

Characterization of the C-Terminal DLQ Motif. The possible role of this motif was investigated by testing the biopotency of PF4 peptides in which the DLQ motif was either deleted or modified (Table 1B). Deletion of the C-terminal Asp^54−Pro^58 resulted in a marked attenuation, by a factor of 30, of the inhibitory potency of the truncated peptide PF4(34−53) on the proliferation of CFU-MK (Figure 5), as well as on the other hematopoietic progenitors CFU-GM and BFU-E (results not shown). The reduced activity of this peptide was essentially attributed to the deletion of the DLQ motif, because the peptide PF4(34−56) which contains this motif inhibited the formation of hematopoietic colonies at concentrations similar to that of the reference PF4(34−58) (Figure 5). Replacement of the DLQ motif by DLE or DLN decreased the capacity of modified peptides to inhibit the proliferation of hematopoietic progenitors (Figure 5). When compared to the reference peptide, 30-fold higher concentrations of the peptide containing the DLE modification were required to obtain the same inhibitory effect. In contrast, the modification of DLQ to DLN completely abolished the activity of PF4(34−58), at least for a 650 nM concentration, which is 30-fold higher than the reference concentration for PF4(34−58). Given that the predicted helicity of those PF4(34−58) peptide derivatives with a deleted or modified DLQ motif was not expected to change compared to the reference peptide (Figure 2D), this demonstrates that the chemokine-specific DLQ motif plays a specific role in peptide PF4(34−58) activity on the progenitor cells. In particular, the charge and/or the volume of residue side chain in position 56 (Gln^56) appeared to be required for the recognition of the DLQ motif or for its interaction with a putative receptor.

Functional Cooperation between the N- and C-Terminal Motifs. The above results show that both the predicted α-helix element and the DLQ motif are required for full hematopoietic inhibitory activity of the chemokine-derived PF4(34−58). The functional relationship between the helical unit and the DL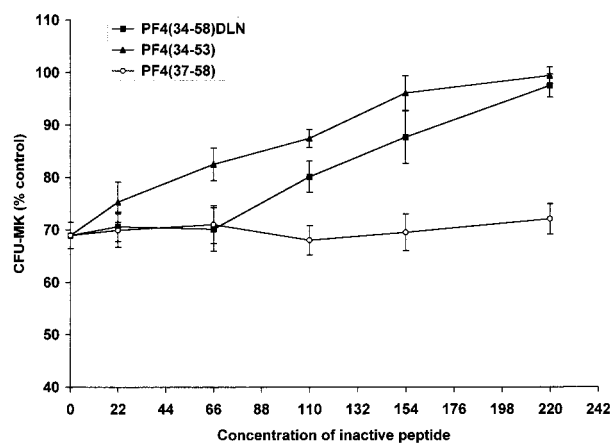Q motif was examined in a competition assay for suppression of progenitor proliferation in vitro (Figure 6). A mixture of the native PF4(34−58) peptide (22 nM) and an excess of an inactive peptide (22−220 nM), resulting from a depressed helicity or a deleted DLQ motif, was added to the cultures. The peptide PF4(34−53), from which the DLQ motif was deleted, competed in a dose-dependent manner with the reference peptide PF4(34−58). A competition value of 50% was achieved at doses as low as 110 nM of peptide PF4(34−53) which corresponds to a 1:5 ratio for active:inactive peptide. Moreover, inhibition of CFU-MK proliferation by PF4(34−58) was fully abolished by a 10-fold excess of PF4(34−53). Interestingly, the peptide PF4-(34−58)DLN was also able to compete with the reference peptide PF4(34−58) as the truncated PF4(34−53). Indeed, half and full competitions were observed at 1:5 and 1:10 ratios for active:inactive peptide, respectively. In contrast, the peptides PF4(37−58) and PF4(37−56), with the intact DLQ motif but a decreased helicity, were not able to interfere with the activity of the reference peptide. No competition was observed, even at a 220 nM concentration of PF4(37−58),which corresponds to a 1:10 ratio of active versus inactive peptide.

Conformational Analysis of Modified PF4(34−58) Peptides. To provide structural support for these in vitro and predictive data, the PF4(34−58) peptide derivatives were analyzed by CD, FTIR, and NMR spectroscopies at low TFE concentrations.

CD Analysis. The far-UV CD spectra of all PF4 analogues recorded in TFE (≤10%), pH 7.0, 20 °C (Figure 7A) displayed a weak minimum at 222 nm (α-helices) and a strong minimum at 200 nm (unordered structures). Addition of 25% TFE strongly modified the profile of these CD spectra (Figure 7B), because molar ellipticity decreased at both 208 and 222 nm and increased at 190 nm, reflecting the stabilization of ordered structures over the random-coil structures (37).

The estimation of secondary structures from CD spectra of those PF4 peptides were performed by using different
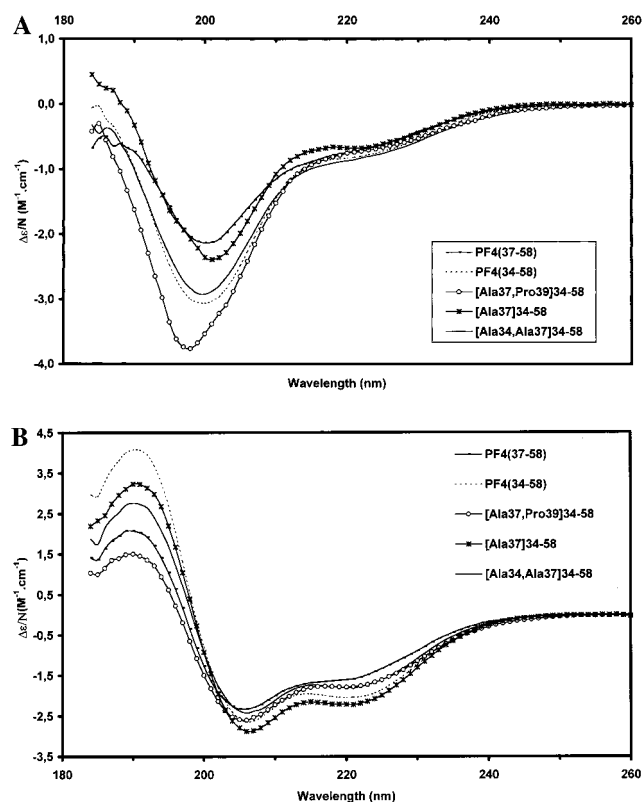
FIGURE 7: CD spectra of PF4(34−58) peptides. Far-UV CD spectra of peptides in H_2O (A) and 25% TFE (B) are shown as mean molar residue ellipticity ($\Delta\epsilon/N$) versus wavelength (nm). Measurements were performed at 25 °C for a 40 μM concentration of peptides.

Table 2: Relative Abundance of Secondary Structure Elements in PF4(34−58) Analogues[a]

peptides	α-helix	β-sheet	β-turn	aperiodic
PF4(37−58)	13	42	5	40
PF4(34−58)	20	36	4	40
[Ala^{37},Pro^{39}](34−58)	15	27	14	44
[Ala^{37}](34−58)	19	35	6	40
[Ala^{34},Ala^{37}](34−58)	18	35	5	42

[a] The numbers shown were calculated from CD spectra recorded in aqueous TFE/H_2O (25%) using 5 methods as described in Experimental Procedures (18). Although intrinsic values varied from one evaluation method to another, the variation observed within each peptide was always the same.

methods (Table 2). Unexpectedly, the data indicated that the modifications produced only a slight change in the secondary structures of the PF4(34−58) peptides. However, it could be observed that peptides with a reduced biological activity, peptides [Ala^{37},Pro^{39}](34−58) and PF4(37−58), were characterized by a low percentage of α-helix and also by different percentages of β-sheet as compared to other PF4(34−58) analogues.

FTIR Analysis. Figure 8A−E shows the infrared spectra of PF4(34−58) peptides (25% TFE-d_2/D_2O) obtained in the 1700−1500 cm^{-1} region (amide I and II bands) and also the component spectral bands that are used to fit the spectrum of each peptide. For the analysis of the privileged secondary structures adopted by the PF4(34−58) analogues, only the more informative amide I band was analyzed (20).

Figure 8A−E reveals that the broad amide I contour of each spectrum is composed of eight bands at 1696, 1683, 1672, 1662, 1651, 1636, 1626, and 1617 cm^{-1}. On the basis

Table 3: Frequency and Quantitative Contribution of Each Component Spectral Band to the Total Amide I Contour of Each PF4(34−58) Analogue[a]

[Ala^{34},Ala^{37}] (34−58)	[Ala^{37},Pro^{39}] (34−58)	PF4 (34−58)	PF4 (34−53)	PF4 (37−58)
1682	1682	1682	1682	1682
(1.5)	(5.5)	(3.0)	(3.0)	(2.0)
1670	1672	1672	1674	1672
(23.0)	(11.0)	(14.0)	(8.5)	(17.0)
1660	1662	1661	1662	1661
(9.0)	(16.0)	(17.7)	(24.0)	(14.0)
1650	1651	1650	1648	1650
(32.0)	(21.5)	(25.5)	(30.0)	(32.5)
1638	1637	1638	1637	1637
(16.0)	(38.5)	(28.5)	(17.0)	(24.5)
1628	1627	1627	1628	1627
(18.0)	(7.0)	(11.5)	(16.5)	(10.0)

[a] The numbers indicated in parentheses represent the percentage of each component calculated from FTIR spectra recorded in aqueous TFE/H_2O (25%) using curve-fitting procedures (20−23).

Table 4: Helical Content of PF4(34−58)-Derived Peptides[a]

peptides	% α-helix
PF4(37−58)	15
PF4(34−58)	25
[Ala^{34},Ala^{37}](34−58)	26
PF4(34−53)	35
PF4(37−56)	20

[a] The percentage values of α-helix were determined from NMR experiments performed on peptides in aqueous TFE/H_2O (20%) by using the method described in Experimental Procedures (30).

of several studies of peptide chains in proteins and peptides (20−23), the assignment of these bands can be summarized as follows: The 1626 and 1636 cm^{-1} components are generally attributed to β-sheet structures (21, 41, 42), whereas the bands in the 1690−1670 cm^{-1} region contain contributions from both turns or bends and β-sheet structures (43−45). However, on the basis of FTIR studies of both model polypeptides and proteins with very high β-sheet contents (42, 46−48), it can be deduced that the bands around 1683 and 1673 cm^{-1}, together with the band at 1663 cm^{-1}, are indicative of residues engaged in turns or bends as well as of α-type helical structures with distorted hydrogen bonding (45, 49, 50). The amide I band at 1651 cm^{-1} arises generally from α-helices (21, 51). The remaining bands, situated outside the amide I region, are due to specific vibrations of amino acid side chains (46, 52, 53).

Table 3 summarizes the contribution of each band to the total amide I contour determined by curve-fitting procedures (20−23). Upon the basis of these data, the analyzed peptides could be classified into 3 groups, as compared to the reference peptide: (i) the peptides PF4(34−53) and [Ala^{34},Ala^{37}]-(34−58), which are characterized by high proportions for both the 1651 and 1672 or 1662 cm^{-1} bands and a low percentage for the 1637 cm^{-1} band, (ii) the peptide [Ala^{37},Pro^{39}]-(34−58), which shows a decrease of the 1651 cm^{-1} band and a high percentage of the 1637 cm^{-1} band, and (iii) the peptides PF4(37−58) and PF4(37−56), which exhibit a high increase of the 1651 cm^{-1} band and a minor change in the 1637 cm^{-1} band. These observations can be used to explain the differences observed in the inhibitor properties of these PF4(34−58) analogues.

NMR Analysis. To better characterize the privileged secondary structures adopted by the PF4(34−58) peptide, a
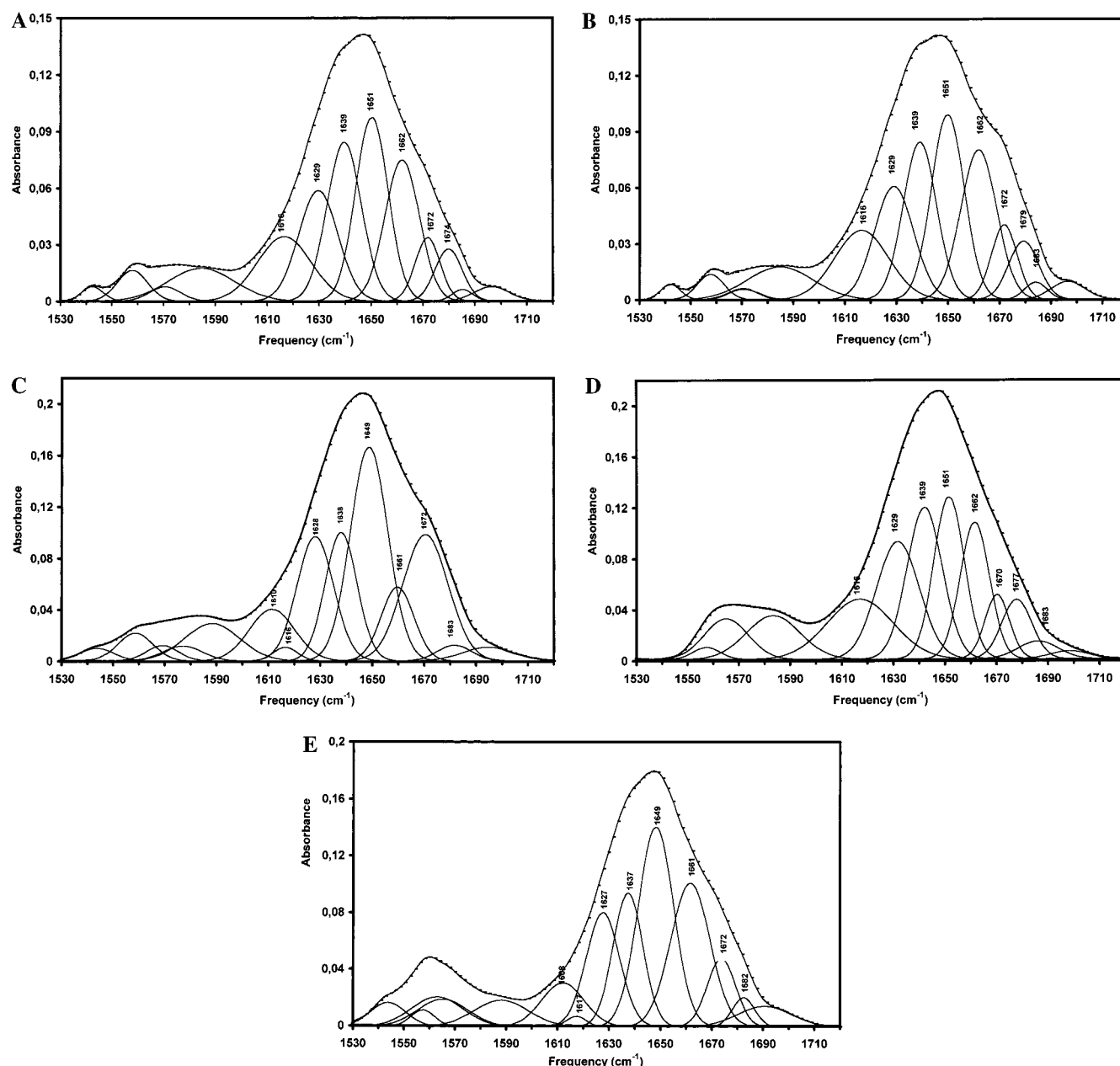
FIGURE 8: The amide I and amide II bands of the FTIR spectra of PF4(34−58) peptide analogues. The measured (- - -) and curve-fitting (—) spectra of peptides PF4(34−58) (A), [Ala[37],Pro[39]](34−58) (B), [Ala[34],Ala[37]](34−58) (C), PF4(37−58) (D), and PF4(34−53) (E) in 25% TFE are shown with the component bands resulting from the analysis (see Experimental Procedures). Measurements at 25 °C in D₂O/TFE-d_2 mixtures (25%) were performed for a 10 mg/mL concentration of peptides.

few PF4(34−58)-derived peptides were analyzed by NMR. Signals were assigned by the standard two-stage procedure outlined by Wüthrich (*54*). From the amide protons, TOCSY experiments allowed identification of almost all the side-chains protons. Their sequential assignments were obtained from NOESY experiments. The detailed chemical-shift assignments are included in the Supporting Information. The presence of a fraction of molecules in an ordered conformation is supported by the analysis of the following NMR parameters: (i) chemical shifts, (ii) coupling constants, and (iii) NOE interactions.

(i) α-Proton secondary chemical shifts obtained for the five peptides are significantly negative throughout the fragment Thr[38]−Lys[46] of peptides PF4(34−58), PF4(34−53), and [Ala[34],Ala[37]](34−58) and for the fragment Ala[39]−Lys[46] of peptides PF4(37−58) and PF4(37−56) (Figure 9). Using the

chemical shift index method (CSI) (*55, 56*), these segments (Thr[38]−Lys[46] and Ala[39]−Lys[46]) must be helical in the 20% TFE:H₂O mixture (Table 4). On the basis of the intensity of the induced shifts, it can be inferred that the stability of the α-helix differs from one peptide to an other. Hence, the peptides could be classified into two groups. The most stable α-helix is found for peptides PF4(34−58), PF4(34−53), and [Ala[34],Ala[37]](34−58), whereas for peptides PF4(37−58) and PF4(37−56), the shorter helix is less stable.

(ii) $^3J_{NH−H\alpha}$ coupling constants are representative of the average conformation in solution. In TFE/H₂O mixtures, RMN line widths are known to be broadened, leading to an overestimation of $^3J_{NH−H\alpha}$ values that is emphasized for small values or to the vanishing of the connectivity peak in the DQF-COSY spectrum. Consequently, $^3J_{NH−H\alpha}$ coupling constants could not be used to determine the length and
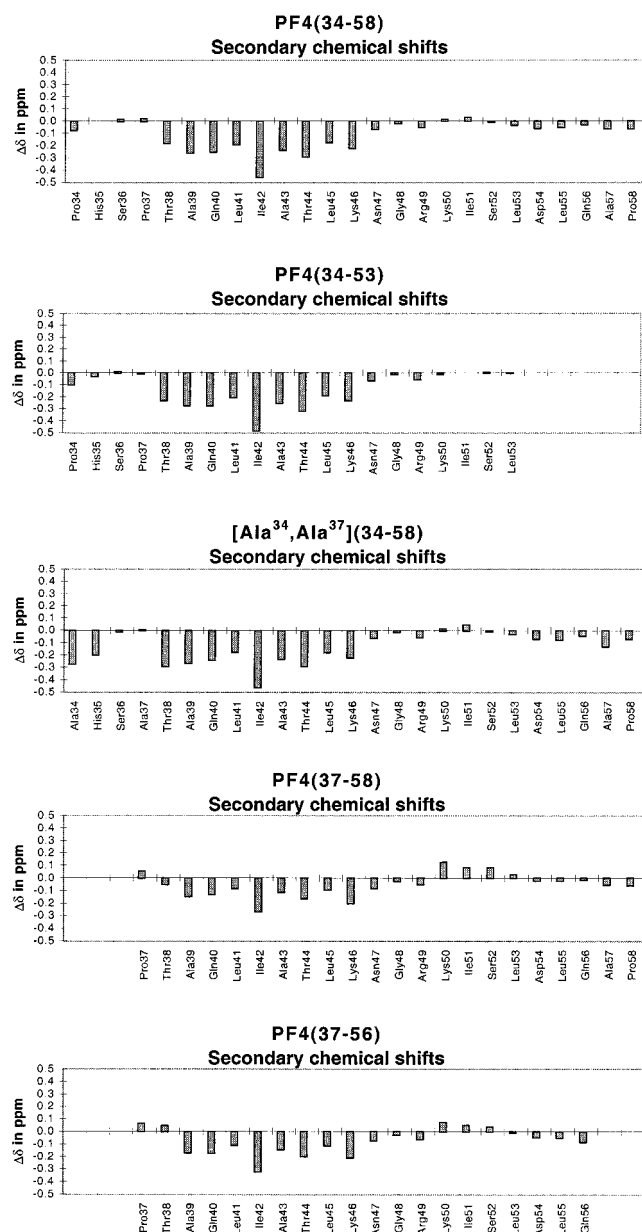
FIGURE 9: Secondary chemical shifts of protons versus sequence for the peptides PF4(34−58), PF4(34−53), [Ala³⁴,Ala³⁷](34−58), PF4(37−58), and PF4(34−56). The chemical shifts of Hα are compared to those chemical shifts of the amino acid in a random coil. As defined by Wishart et al. (*55, 56*), the difference between the random coil values and that of the amino acid in the peptide can indicate the structural environment of that amino acid (α-helix or β-sheet).

the helix stability. However, for all the peptides, except for the peptide PF4(37−56), which could not be further analyzed due to gel formation, smaller $^3J_{NH-H\alpha}$ values are observed for residues Ala³⁹−Asn⁴⁷ of PF4(34−58), for residues Ala³⁷−Lys⁴⁶ of [Ala³⁴,Ala³⁷](34−58), and for residues Ala³⁹−Lys⁴⁶ of PF4(34−53). In the peptide PF4-(37−56), smaller values are measured for residues Ala³⁹−Asn⁴⁷ and Arg⁴⁹−Leu⁵³. These small values of $^3J_{NH-H\alpha}$ may be indicative of partial helical conformation.

(iii) A schematic diagram summarizing the various connectivities observed in the NOESY spectra for the PF4(34−58) peptides in the TFE/H₂O mixture is shown in Figure 10. It can be seen that sequential dNN($i, i+1$) interactions

observed for residues involved in fragments Thr³⁸−Lys⁴⁶ of peptide PF4(34−58) are associated with the presence of medium-range NOEs, such as $d\alpha$N($i, i+3$), $d\alpha\beta$($i, i+3$), and dNN($i, i+2$), that are characteristic of helical conformation.
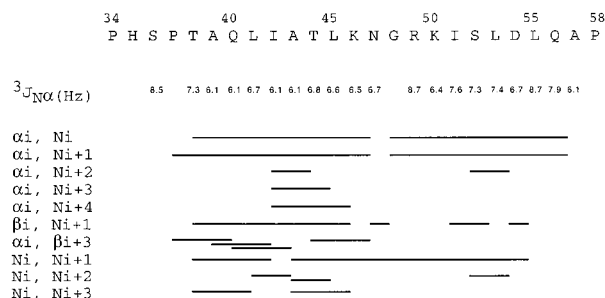
DISCUSSION

Peptides corresponding to different amino acid sequences derived from either the N- or the C-terminal region of PF4, or of other chemokines (*13, 57, 58*), were previously described. Noticeably, the activity of these peptide fragments was found only similar or diminished when compared to the original chemokine. PF4(34−58) was the first chemokine-derived peptide described with increased multilineage inhibition of hematopoietic progenitors (*14*). This peptide, derived from the central region of PF4, impaired myeloid colony formation at concentrations 30−60-fold lower than the intact chemokine molecule. Moreover, the inhibition induced by the peptide PF4(34−58) was independent of the heparin-binding properties of PF4, suggesting a newly found pathway in the suppression of hematopoiesis. By using predictive methods and a combination of spectroscopic techniques to define secondary structure, we have determined structural parameters and defined motifs which appear to be involved in conferring biological activity to this peptide. Moreover, on the basis of these considerations, we were able to design new molecules derived from the PF4(34−58) sequence and with either diminished or enhanced biological potencies in a multilineage assay on hematopoiesis suppression.

The rationale for such an approach was that in the 34−58 fragment of PF4, two successive motifs could be predicted. From the N- to C-terminus, an α-helical stretch spanned from residue Thr³⁸ to residue Lys⁴⁶ and the DLQ(54−56) tripeptide tag situated at the C-terminus of the peptide. The α-helical motif appeared to be functionally essential because modifications of its extent on the N-terminus had significant effects on the inhibitory action of the resulting peptides. A shift of Pro³⁷ to position 39 resulted in a decrease of the helicity of the modified peptide which produced a marked loss of its hematopoietic-suppressive activity. On the other hand, replacement of Pro³⁹ or Pro³⁴ and Pro³⁹ by an alanine in the peptide [Ala³⁷,Pro³⁹](34−58), which seems to favor an extended α-helicity, was accompanied by a significant increase in the biopotency of the new peptide. This supported a correlation between the α-helix of the peptide and its inhibitory effect on the hematopoietic progenitors. Moreover, the stability of this α-helix was dependent upon the Pro³⁴-Xaa-Zaa-Pro³⁷ tetrapeptide motif, because its deletion or truncation from the N-terminal end of the reference peptide led to a complete loss of activity. The importance of this motif was clearly illustrated with peptides PF4(37−58) and PF4(37−56), which were not able to compete with the intact reference peptide sequence in the suppressive bioassay on hematopoietic progenitors. The second motif is the C-terminal DLQ(54−56) tripeptide, whose importance for the activity of the native PF4 has been previously suggested by others (*36*). Indeed, either its modification to DLN or its deletion abolished the biopotency of the original PF4(34−58) peptide. However, the N-terminal α-helical motif deleted from the DLQ tag [peptide PF4(34−53)] was still able to compete with reference peptide PF4(34−58) in the bioassay.
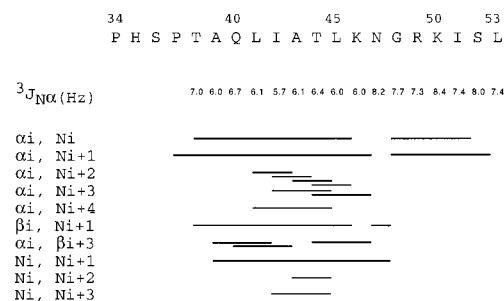
In light of these dual effects, we can conclude that both the α-helical element and the DLQ motif play complemen-
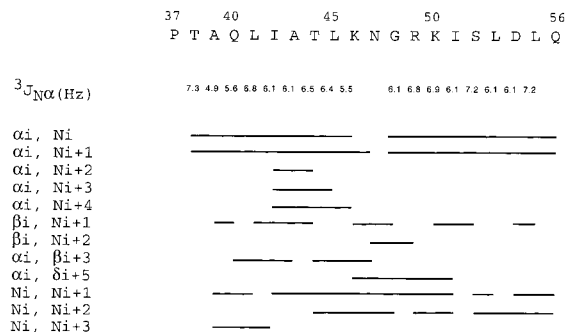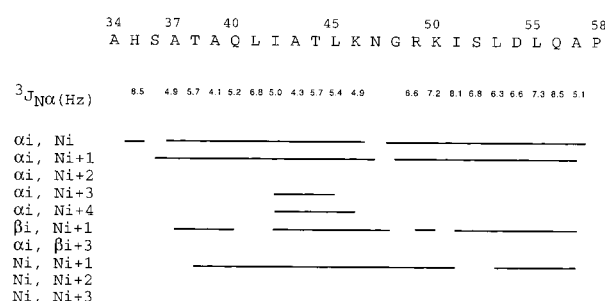
PF4 - $^3J_{N\alpha}$ coupling constants in Hz and NOEs

PF4[34-58]

```
          34       40       45        50        55   58
          P H S P T A Q L I A T L K N G R K I S L D L Q A P

3JNα(Hz)          8.5   7.3 6.1 6.1 6.7 6.1 6.1 6.8 6.6 6.5 6.7   8.7 6.4 7.6 7.3 7.4 6.7 8.7 7.9 6.1

αi, Ni
αi, Ni+1
αi, Ni+2
αi, Ni+3
αi, Ni+4
βi, Ni+1
αi, βi+3
Ni, Ni+1
Ni, Ni+2
Ni, Ni+3
```

PF4[34-53]

```
          34       40       45        50    53
          P H S P T A Q L I A T L K N G R K I S L

3JNα(Hz)         7.0 6.0 6.7  6.1  5.7 6.1 6.4 6.0  6.0 8.2 7.7 7.3  8.4 7.4 8.0 7.4

αi, Ni
αi, Ni+1
αi, Ni+2
αi, Ni+3
αi, Ni+4
βi, Ni+1
αi, βi+3
Ni, Ni+1
Ni, Ni+2
Ni, Ni+3
```

PF4 - $^3J_{N\alpha}$ coupling constants in Hz and NOEs

PF4(37-56)

```
          37    40       45        50      56
          P T A Q L I A T L K N G R K I S L D L Q

3JNα(Hz)        7.3 4.9 5.6 6.8 6.1 6.1 6.5 6.4 5.5    6.1 6.8 6.9 6.1 7.2 6.1 6.1 7.2

αi, Ni
αi, Ni+1
αi, Ni+2
αi, Ni+3
αi, Ni+4
βi, Ni+1
βi, Ni+2
αi, βi+3
αi, δi+5
Ni, Ni+1
Ni, Ni+2
Ni, Ni+3
```

[Ala34,Ala37](34-58)

```
          34    37    40       45        50        55   58
          A H S A T A Q L I A T L K N G R K I S L D L Q A P

3JNα(Hz)     8.5   4.9 5.7 4.1 5.2 6.8 5.0 4.3 5.7 5.4 4.9    6.6 7.2 8.1 6.8 6.3 6.6 7.3 8.5 5.1

αi, Ni
αi, Ni+1
αi, Ni+2
αi, Ni+3
αi, Ni+4
βi, Ni+1
αi, βi+3
Ni, Ni+1
Ni, Ni+2
Ni, Ni+3
```

FIGURE 10: Summary of ^{1}H$-^1$H NOE connectivities and $^3J_{NH-H\alpha}$ connectivities obtained for the PF4(34−58) peptides.

tary roles for the expression of full hematopoietic inhibitory activity of the PF4(34−58) chemokine-derived peptides. Considering that (i) among the inactive peptides, that is, PF4(34−53), PF4(37−58), and PF4(37−56), only peptide PF4(34−53) deleted of the DLQ motif competes with the reference peptide, and (ii) this peptide has a helix length and stability comparable to that of peptides PF4(34−58) and [Ala^{34},Ala^{37}](34−58), it could be hypothesized that the α-helical segment might be essential for interaction with a putative receptor site, while the DLQ motif might possibly participate in the direct activation of this receptor. Noticeably, a similar two-step model has been proposed for the inter-action of IL8 with its receptors (59). Several groups have reported that this chemokine contains two domains important for its activity. One of these sequences corresponds to the ELR motif (8, 60), which may play a role similar to that of DLQ (36). A cluster of hydrophobic residues participates in IL8 recognition for IL8 receptors and may be essential for receptor binding affinity (61, 62).

In the three-dimensional structure of native PF4, the PF4-(34−58) sequence is implicated in a β-sheet (7). However, in this work we found that in the presence of low TFE concentrations, the corresponding peptide fragment adopts an α-helical structure in its central region. It is now established that addition of low-TFE-percentage:water solu-tion to peptides favors sample organizations with conforma-tions which are dictated by their amino acid sequences. It should be kept in mind that TFE does not simulate the protein environment (63). This α-helix organization, already ob-served for other PF4 analogues which correspond to peptide segments adopting a β-sheet structure in the native molecule (64, 65), is possibly due to hydrophobic interactions (66) or to the absence of the partner strand (63).

It is worth noting that the three-dimensional structure of native PF4 indicates a fold consisting of a C-terminal α-helix preceded by three antiparallel β-sheets in the central region (7). Moreover, the DLQ motif at position 54−56 is located very close to the α-helix formed by the C-terminal residues 61−70. Because PF4(34−58) presents an inhibitory activity which is more potent than native PF4 (14), it can be concluded that the peptide PF4(34−58) may mimic a cluster of functional sites in PF4 characterized by the proximity of a DLQ motif to an α-helix.

Modeling of peptide PF4(34−58) may in the future indicate whether the relative position of the defined func-tional parameters is similar to the cluster in the native chemokine. This will allow the design of new synthetic chemokine mimetics with highly suppressive multilineage activity on hematopoiesis. On the other hand, mimetics lacking the DLQ motif should also be considered in the design of molecules with antagonistic activity.

ACKNOWLEDGMENT

SUPPORTING INFORMATION AVAILABLE

Tables of ^{1}H NMR data. This material is available free of charge via the Internet at http://pubs.acs.org.

REFERENCES

1. Rollins, B. J. (1997) *Blood 90*, 909−928.
2. Broxmeyer, H. E., Sherry, B., Lu, L., Cooper, S., Oh, K. O., Tekamp-Olson, P., Kwon, B. S., and Cerami, A. (1990) *Blood 76*, 1110−1116.

3. Graham, G. J., Wright, E. G., Hewick, R., Wolpe, S. D., Wilkie, N. M., Donaldson, D., Lorimore, S., and Pragnell, I. B. (1990) *Nature 344*, 442−444.

4. Han, Z. C., Sensèbe, L., Abgrall, J. F., and Brière, J. (1990) *Blood 75*, 1234−1239.

5. Sarris, A. H., Broxmeyer, H. E., Wirtmueller, U., Karasavvas, N., Cooper, S., Lu, L., Krueger, J., and Ravetch, J. V. (1993) *J. Exp. Med. 178*, 1127−1132.

6. Clore, G. M., and Gronenborn, A. M. (1991) *J. Mol. Biol. 217*, 611−620.

7. Zhang, X., Chen, L., Bancroft, D. P., Lai, C. K., and Maione, T. E. (1994) *Biochemistry 33*, 8361−8366.

8. Hebert, C. A., Vitangcol, R. V., and Baker, J. B. (1991) *J. Biol. Chem. 266*, 18989−18994.

9. LaRosa, G. J., Thomas, K. A., Kaufmann, M. E., Mark, R., White, M., Taylor, L., Gray, G., Witt, D., and Navarro, J. (1992) *J. Biol. Chem. 267*, 25402−25406.

10. Moser, B., Dewald, B., Barella, L., Schmacher, C., Baggiolini, M., and Clark-Lewis, I. (1993) *J. Biol. Chem. 268*, 7125−7128.

11. Wells, T. N. C., Power, C. A., and Proudfoot, A. E. I. (1998) *Trends Pharmacol. Sci. 19*, 376−380.

12. Szabo, M. C., Soo, K. S., Zlotnik, A., and Schall, T. J. (1995) *J. Biol. Chem. 270*, 25348−25351.

13. Clark-Lewis, I., Dewald, B., Geiser, T., Moser, B., and Baggiolini, M. (1993) *Proc. Natl. Acad. Sci. U.S.A. 90*, 3574−3577.

14. Lecomte-Raclet, L., Alemany, M., Sequeira-Le Grand, A., Amiral, J., Quentin, G., Vissac, A. M., Caen, J. P, and Han, Z. C. (1998) *Blood 91*, 2772−2780.

15. Stewart, J. M., and Young, J. D. (1984) in *Solid-Phase Peptide Synthesis.* 2nd ed., p 135, Pierce Chemical Co., Rockford, IL.

16. Lecomte-Raclet, L., Aidoudi, S., Lebeurier, I., Bal dit Solier, C., Kishtoo, G., Aubert, J. F., Caen, J. P., and Han, Z. C. (1998) *Platelets 9*, 121−127.

17. Muñoz, V., and Serrano, L. (1994) *Nat. Struct. Biol. 1*, 399−409.

18. Venyaminov, S. Y., and Yang, J. T. (1996) *Circular Dichroism and the Conformational Analysis of Biomolecules* (Fasman, G. D., Ed.) Plenum Press, New York, London.

19. Moriaty, D. F., and Raleigh, D. P. (1999) *Biochemistry 38*, 1811−1818.

20. Surewicz, W. K., Mantsch, H. H., and Chapman, D. (1993) *Biochemistry 32*, 389−394.

21. Byler, D. M., and Susi, H. (1986) *Biopolymers 25*, 469−487.

22. Bandekar, J. (1992) *Biochim. Biophys. Acta 1120*, 123−143.

23. Jackson, M., and Mantsch, H. H. (1995) *Crit. Rev. Biochem. Mol. Biol. 30*, 35−120.

24. Zuiderweg, E. R., Hallenga, K., and Olejniczak, E. T. (1986) *J. Magn. Reson. 70*, 336−343.

25. States, D. J., Haberkorn, R. A., and Ruben, D. J. (1982) *J. Magn. Reson. 48*, 286−292.

26. Rance, M., Sorensen, O. W., Bodenhausen, G., Wagner, G., Ernst, R. R., and Wüthrich, K. (1983) *Biochem. Biophys. Res. Commun. 117*, 479−485.

27. Bax, A., and Davis, D. (1985) *J. Magn. Reson. 65*, 355−360.

28. Griesinger, C., Otting, G., Wüthrich, K., and Ernst, R. R. (1988) *J. Am. Chem. Soc. 110*, 7870−7872.

29. Macura, S., Huang, Y., Suter, D., and Ernst, R. R. (1981) *J. Magn. Reson. 43*, 259−281.

30. Wishart, D. S., and Sykes, B. D. (1994). *Methods Enzymol. 239*, 363−393.

31. Ciaglowski, R. E., Snow, J., and Walz, D. A. (1986) *Arch. Biochem. Biophys. 250*, 249−256I.

32. Doi, T., Greenberg, S. M., and Rosenberg, R. D. (1987) *Mol. Cell. Biol. 7*, 898−904.

33. Poncz, M., Surrey, S., LaRocco, P., Weiss, M. J., Rappaport, E. F., Conway, T. M., and Schwartz, E. (1987) *Blood 69*, 219−223.

34. St. Charles, R., Walz, D. A., and Edwards, B. F. P. (1989) *J. Biol. Chem. 264*, 2092−2099.

35. Shigeta, O., Lu, W. Q., Holt, J. C., Edmunds, L. H., Jr, and Niewiarowski, S. (1991) *Thromb. Res. 64*, 509−520.

36. Daly, T. J., LaRosa, G. J., Dolich, S., Maione, T., Cooper, S., and Broxmeyer, H. E. (1995) *J. Biol. Chem. 270*, 23282−23292.

37. Woody, R. W. (1995) *Methods Enzymol. 246*, 34−47.

38. MacArthur, M. W., and Thornton, J. M. (1991) *J. Biol. Chem. 218*, 397−412.

39. Brakch, N., Boileau, G., Simonetti, M., Nault, C., Joseph-Bravo, P., Rholam, M., and Cohen, P. (1993) *Eur. J. Biochem. 216*, 39−47.

40. Vanhoof, G., Goossens, F., De Meester, I., Hendriks, D., and Scharpe, S. (1995) *FASEB J. 8*, 736−744.

41. Dong, A., Huang, P., and Caughey, W. (1990) *Biochemistry 29*, 3303−3308.

42. Kalnin, N. N., Baikalov, I. A., and Venyaminov, S. Yu. (1990) *Biopolymers 30*, 1273−1280.

43. Halverson, K., Fraser, P., Kirschner, D., and Lansbury, P. (1990) *Biochemistry 29*, 2639−2644.

44. Prestrelski, S., Byler, D., and Liebman, M. (1991) *Biochemistry 30*, 133−143.

45. Kennedy, D., Crisma, M., Toniolo, C., and Chapman, D. (1991) *Biochemistry 30*, 6541−6548.

46. Arrondo, J., Young, N., and Mantsch, H. (1988) *Biochim. Biophys. Acta 952*, 261−268.

47. Casal, H. L., Kohler, U., and Mantsch, H. H. (1988) *Biochim. Biophys. Acta 957*, 11−20.

48. Dousseau, F., and Pézolet, M. (1990) *Biochemistry 29*, 8771−8779.

49. Krimm, S., and Bandekar, J. (1986) *Adv. Protein Chem. 38*, 181−364.

50. Urbanova, M., Dukor, R. K., Pancoska, P., Gupta, V. P., and Keiderling, T. A. (1991) *Biochemistry 30*, 10479−10485.

51. Holloway, P., and Mantsch, H. (1989) *Biochemistry 28*, 931−935.

52. Chirgadze, Y., Fedorov, O., and Trushina, N. (1975) *Biopolymers 14*, 679−694.

53. Venyaminov, S., and Kalnin, N. (1990) *Biopolymers 30*, 1243−1257.

54. Wüthrich, K. (1986) *NMR of Protein and Nucleic Acids*, Wiley Interscience, J. Wiley, New York.

55. Wishart, D. S., Sykes, B. D., and Richards, F. M. (1991) *J. Mol. Biol. 222*, 311−333.

56. Wishart, D. S., Sykes, B. D. and Richards, F. M. (1992) *Biochemistry 31*, 1647−1651.

57. Hayashi, S. (1995) *J. Immunol. 154*, 814−824.

58. Lebeurier, I., Basara, N., Aidoudi, S., Amiral, J., Caen, J. P., and Han, Z. C. (1996) *Br. J. Haematol. 92*, 29−34.

59. Wuu, L., Ruffing, N., Shi, X., Newman, W., Soler, D., Mackay, C. R., and Qin, S. (1996) *J. Biol. Chem. 271*, 31202−31209.

60. Clark-Lewis, I., Dewald, B., Loetscher, P., Moser, B., and Baggiolini, M. (1994) *J. Biol. Chem. 269*, 16075−16081.

61. Hammond, M. E. W., Shyamala, V., Siani, M. A., Gallegos, C. A., Feucht, P. H., Abbott, J., Lapointe, G. R., Moghadam, M., Khoja, H., Zakel, J., and Tekamp-Olson, P. (1996) *J. Biol. Chem. 271*, 8228−8235.

62. Williams, G., Borkakoti, N., Bottomley, G. A., Cowan, I., Fallowfield, A. G., Jones, P. S., Kirtland, S. J., Price, G. J., and Price, L. (1996) *J. Biol. Chem. 271*, 9579−9586.

63. Sönnichson, F. D., Van Eyk, J. E., Hodges, R. S., and Sykes, B. D (1992) *Biochemistry 31*, 8790−8798.

64. Ilyina, E., Milius, R., and Mayo, K. H. (1994) *Biochemistry 33*, 13436−13444.

65. Daragan, V. A., Ilyina, E., Fields, C. G., Fields, G. B., and Mayo, K. H. (1997) *Protein Sci. 6*, 355−363.

66. Chan, H. S., and Dill, K. A. (1990) *Proc. Natl. Acad. Sci. U.S.A. 87*, 6388−6392.